

Density Functional Theory Calculations in Designing Symmetric and Asymmetric TADF Emitters*

Dalius Gudeika^{1,*}

¹ Vilnius University, Akademijos Str. 4, 08412, Vilnius, Lithuania

Abstract

A pair of thermally activated delayed fluorescence (TADF) emitters with symmetric and asymmetric D-A-D structure are investigated. The introduction of density functional theory (DFT) has tremendously aided the application of computational material science in the design and development of organic materials. The use of DFT and other computational approaches avoids time-consuming empirical processes. Therefore, this review explored how the DFT computation may be utilized to explain some of the features of organic systems. First, we went through the key aspects of DFT and provided some context. Then we looked at the essential characteristics of an organic system that DFT simulations could predict. Gaussian software had been employed with the B3LYP functional and 6-31G(d, p) basic sets for organic systems.

Keywords

DFT, TADF emitters, B3LYP, 6-31G(d, p) basic sets

1. Introduction

The TADF mechanism is based on a second-order spin-vibronic coupling between a charge transfer triplet state (³CT) and a local excited triplet (³LE) to mediate the up-conversion reverse intersystem crossing (rISC) of the coupled ³LE/³CT triplet(s) to the emissive charge transfer singlet (¹CT) state [1]. Building on the previous findings [2] and aiming to better understand the connection between analogous D-A and D-A-D molecules, we investigate two isomeric D-A-D TADF emitters comprised of a benzonitrile acceptor and acridine donors attached at the 2,5- or 2,6- positions of the acceptor. Comparison to previously reported D-A materials (facilitated by the self-regulating dihedral angle of DMAC) allows us to compare these systems with minimal additional complexity introduced by the second D unit. Using a combination of experimental and theoretical methods, it was demonstrated that electronic interaction between the donating moieties – modulated by the relative position of each – alters the ³LE energy and thus also ΔE_{ST} and TADF performance.

Computational methodologies, such as DFT, have been developed to bypass time-consuming empirical procedures for the optimization of these formulations.

DFT computations, in particular, offer outstanding levels of accuracy with comparable computation time and are more inexpensive in terms of computational resources than other ab initio approaches currently in use. Additionally, it avoids the many electron wave function in favor of electron density, and has the potential benefit of dealing with only one function of a single spatial coordinate. Moreover, it employs generalized gradient approximations (GGAs), which use the density gradient to generate a more precise function [3].


DFT are a strong and low-cost method for revealing a material's fundamental information, including energy, geometric structure, electrical, and optical characteristics. It offers important theoretical predictions and assistance from the standpoint of material design. It provides crucial information at the levels of atoms, molecules, and unit cells from the perspective of interpreting the results. The influence of element doping on the geometric and electrical characteristics of organic compounds carriers, as well as the interaction between the molecules and the nanocarriers, is considerably aided by DFT calculations [4].


* IVUS2024: Information Society and University Studies 2024, May 17, Kaunas, Lithuania

^{1*} Corresponding author

[†] These author contributed equally.

gudeika.dalius@gmail.com (D. Gudeika)

 0000-0001-5718-8583 (D. Gudeika)

 © 2024 Copyright for this paper by its authors. Use permitted under Creative Commons License Attribution 4.0 International (CC BY 4.0).

2. Experimental section

2.1. Related Works

DFT calculation is a primary tool in predicting and investigating excited state configuration, excited state energy, and molecular geometry of TADF molecules [5]. As with the experimental investigation of TADF molecules, most of the research focuses on excited state configurations and energies of relaxed geometry of excited states and explain experimental phenomena with discrete geometries or excited states such as ^1CT , ^3CT , and ^3LE states. Some researches attempted to relate D-A dihedral angle with S_1 and T_1 energies, but they have several limitations; (1) a large discrepancy with experimental energies due to inappropriate selection of functional, (2) lack of explanation to the effect of dihedral angle to excited state configurations or energies of S_1/T_1 states, or (3) mixed level of theory for S_1 and T_1 leading to inverted S_1/T_1 energies [6]. These problems arise from difficulties in handling triplet states with TD-DFT due to the so-called triplet instability stemming from the exchange-interaction-sensitive nature of triplet states [7].

2.2. Methodology

Quantum chemical calculations of studied derivatives were performed using DFT and TD-DFT implemented in the Gaussian 16 [8] software package. Geometry optimization was provided by means of density functional CAM-B3LYP method and 6-31g(d,p) basis set in the ground S_0 state as well as the lowest excited S_1 state [9].

3. Results and Discussion

3.1. DFT Calculations

To better understand the behaviour of organic compounds we turn to DFT calculations. Figure 1 shows the NTOs and energies calculated for relevant triplet and singlet states in $(o,m)\text{ACA}$ and $(o,o)\text{ACA}$. By inspecting the singlet NTOs in $(o,m)\text{ACA}$ we first note that the CT singlet associated with the *ortho*-donor (S_1) is lower in energy than that associated with the *meta*-donor CT state (S_2). This is in agreement with expectations and the trends established for *oDA* and *mDA*. In $(o,o)\text{ACA}$ the S_1 and S_2 states are much closer in energy, and each involves both of the *ortho*-donor units. These represent symmetric (S_1) and antisymmetric (S_2) combinations of otherwise degenerate CT states associated with either the left or right donor individually. This is analogous to the formation of symmetric (bonding) and antisymmetric (antibonding) molecular orbitals from combinations of degenerate atomic orbitals (Figure 2a). For the first two triplet states of CT nature similar trends are observed.

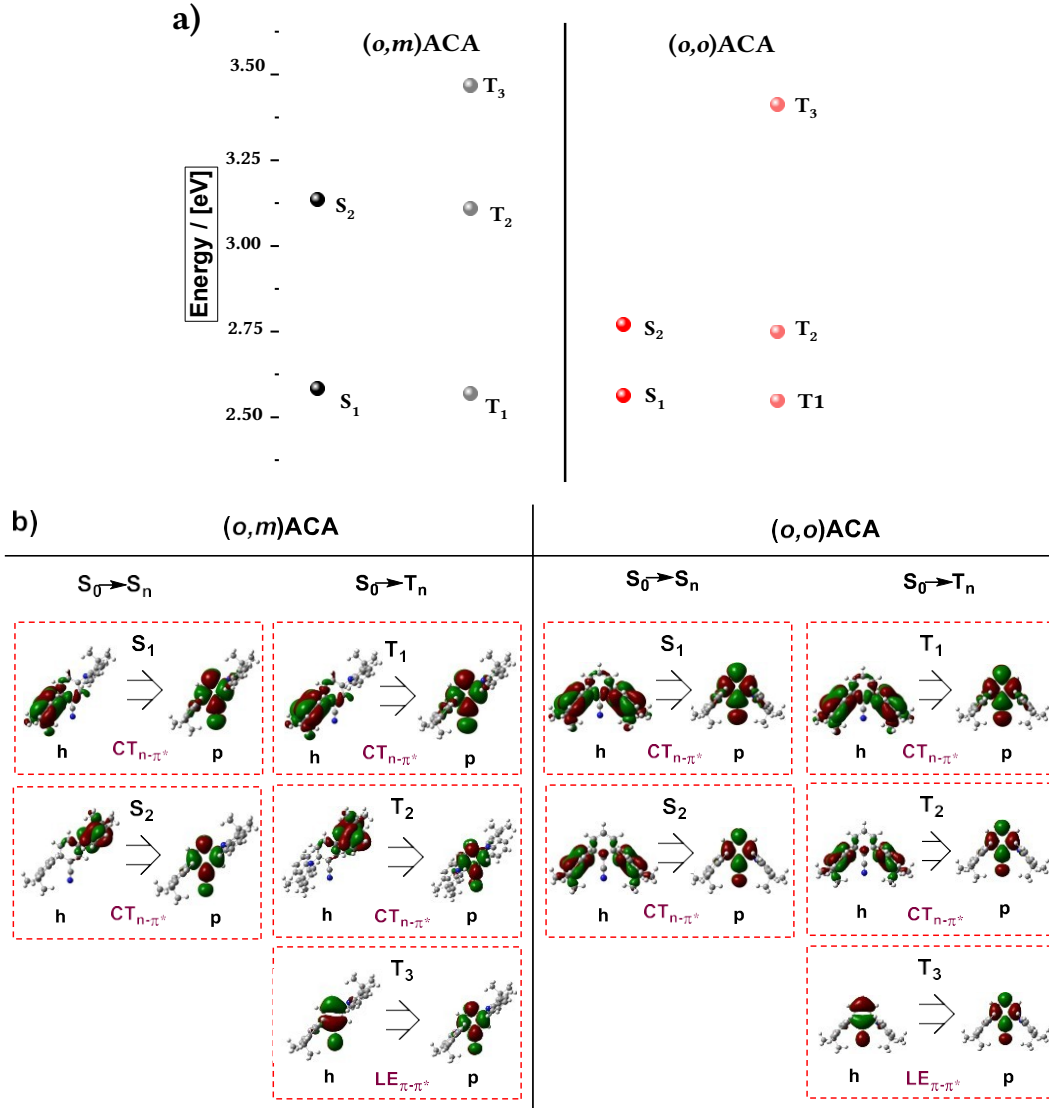


Figure 1: a) Adiabatic singlet / triplet energy diagram of (o,m) ACA and (o,o) ACA (TDA-DFT rBMK/6-31G(d)); b) selected set of natural transition orbitals (NTO) of (o,m) ACA and (o,o) ACA (TDA-DFT rBMK/6-31G(d)) (isovalue = 0.01).

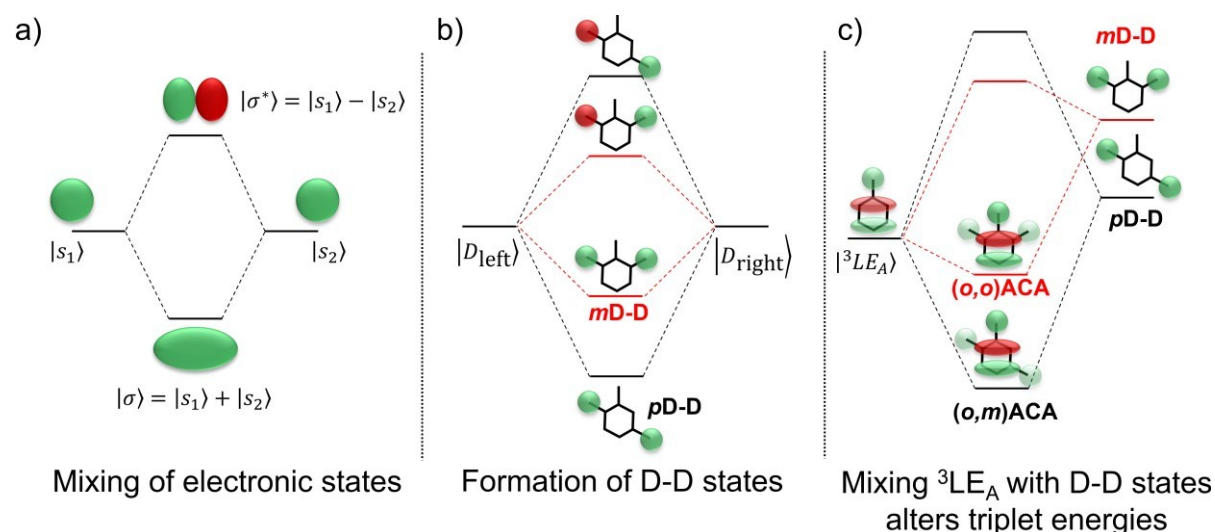
The first triplet state of LE nature is T_3 , centred on the A unit in both materials and with nearly identical NTOs. This LE triplet state is the one relevant to vibronic coupling and rISC. Interestingly, the calculated T_3 energies of (o,m) ACA and (o,o) ACA are in the opposite order as found experimentally, with about the same difference in triplet energies in both cases (~ 50 meV). The reason for the experimental (o,m) ACA triplet energy being lower than (o,o) ACA cannot be due to the combination of individual couplings of the A to the two D units. The two materials to either have identical triplet energies (from coupling between the A and the *ortho*-D in each material), or for (o,m) ACA to have a higher triplet energy than (o,o) ACA (due to coupling between A and *meta*-D, which is intrinsically higher in energy as in *mDA*). Any such state-mixing between LE and CT states is also unlikely to be a contributing factor, due to the forbidden nature of mixing these states with different orbital symmetries [10].

The LE T_3 states in both (o,m) ACA and (o,o) ACA interact with higher-lying LE states delocalised across both donor units (D-D states). A representative state diagram is presented in Figure 2b, showing how these unoccupied electronic states would form.

The proposed D-D states are formed by linear combinations of the individual donor LE states (Figure 2b), and so one of these D-D states (the symmetric combination) is expected to be the lowest-

energy LE singlet state in each molecular system. These D-D states are also unoccupied, which explains why the DFT calculations are unable to accurately predict the order of (o,m) ACA and (o,o) ACA T_3 energies compared to experiment. Accurately accounting for such interactions with unoccupied states would instead require more advanced multireference or complete active space *ab-initio* methods, which are impractical for molecules of this size.

Applying molecular orbital theory in the symmetric and asymmetric D-A-D systems, we can infer several properties of the D-D states and how they would differ. Due to different conjugation strengths across the linker unit for (o,m) ACA (p D-D state) than for (o,o) ACA (m D-D state), the p D-D state to be lower in energy and have larger electron density on the central bridge region (Figure 2b). This would subsequently lead to a larger overlap between the p D-D state and the 3LE state associated with the A unit (3LE_A) in (o,m) ACA as compared to m D-D in (o,o) ACA. The resulting state mixing between D-D and 3LE_A states lowers the observed phosphorescence energies in both materials compared to calculations, which cannot account for interactions with unoccupied orbitals. Due to increased orbital overlap the state mixing with the 3LE_A is more extensive for p D-D than for m D-D, leading to a yet lower triplet energy in (o,m) ACA and the observed ordering of experimental phosphorescence energies (Figure 2c). While other higher-energy LE states would also be influenced by interactions with the D-D states, none of these higher LE states are measured or expected to influence the TADF properties. Due to differences in orbital symmetry the CT states are not expected to interact with the D-D states, and so are totally unaffected both in calculations and



experiment.

Figure 2: State diagrams showing: a) Formation of symmetric and antisymmetric molecular orbitals from pairs of degenerate atomic orbitals. b) Analogous proposed formation of D-D states with different energies due to stronger or weaker conjugation across *meta*- or *para*- bridges in (o,m) ACA (p D-D) and (o,o) ACA (m D-D). c) Different D-D energies and extents of interaction with the acceptor- centred LE triplet state (3LE_A) lead to different experimental triplet energies. All orbital representations and implied relative state energies are indicative only.

The lower triplet energy in (o,m) ACA is therefore identified as an emergent property of the pair of donors. This lowering of triplet energy is irrelevant to the analogous o DA or m DA materials, and is impossible to predict by considering these fragments in isolation.

Although based on well-established principles of molecular orbital theory, much of the previous explanation is speculative. Nonetheless some evidence for the existence of the proposed D-D states can be found in the experimental absorption spectra (Figure 3).

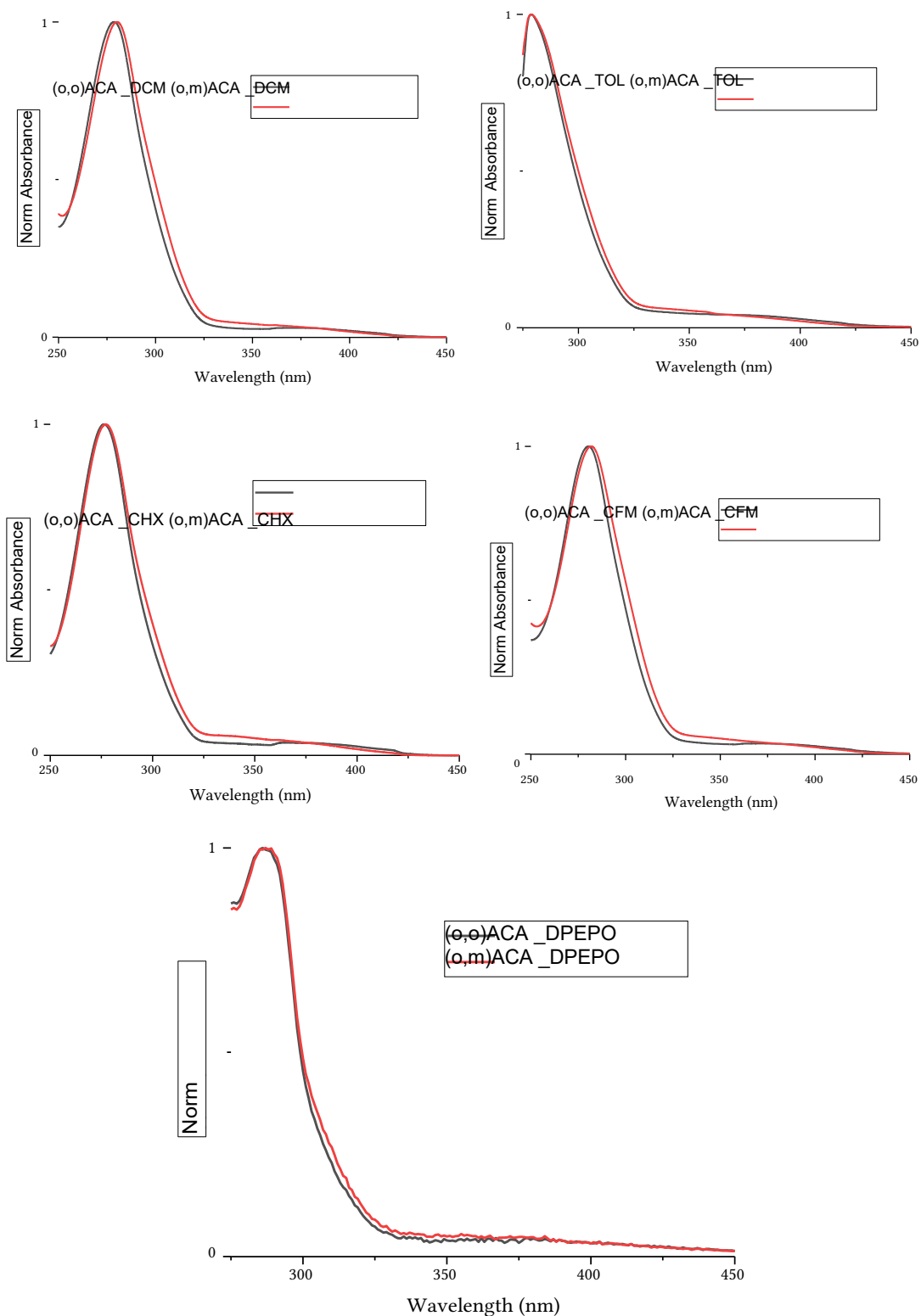


Figure 3: Absorbance spectra in DPEPO films and various dilute solutions (dichloromethane, toluene, cyclohexane, chloroform). The low energy edge of the main donor band is redshifted for $(o,m)ACA$ (~300 to 325 nm) in all cases, attributed to the underlying $pD-D$ state.

In DPEPO films and a range of solvents a redshift in the main absorbance band (peak at ~275 nm, attributed to DMAC) in $(o,m)ACA$ compared to $(o,o)ACA$ was observed. This redshift is due to the presence of a weak underlying band associated with excitation of the $pD-D$ singlet state. In $(o,o)ACA$

the *mD-D* state is expected to exist at higher energies, and therefore remains subsumed by the main donor DMAC absorption band. Furthermore, the absorbance spectra also show the same weak direct CT absorption bands in both (*o,o*)ACA and (*o,m*)ACA at ~375 nm. In each material this band corresponds to two closely spaced CT state absorptions, consistent with the DFT calculations and prior understanding of the *oDA* or *mDA* materials. In both cases this indicates that formation of the CT state involves only a single donor, and is unimpacted by the presence of the other (consistent with both materials sharing the same PL spectrum).

Because (*o,m*)ACA and (*o,o*)ACA introduce minimum additional complexity compared to *oDA* or *mDA*, there are few other explanations aside from D-D interactions that can potentially explain the trends seen here. While an intuitively satisfying example of basic physical chemistry principles in action, these results also demonstrate a new method of control in TADF materials. In contrast to external host-tuning of CT singlet states to minimise ΔE_{ST} , multi-donor interactions may in future be used as a tool to selectively tune triplet states. These results also firmly demonstrate that ‘bottom-up’ approaches to understanding TADF materials are overly simplistic, and that understanding the properties of D-A-D materials purely in terms of their D-A subunits may not be a generally achievable goal.

4. Conclusion

Two D-A-D TADF materials were compared with analogous D-A compounds. Despite displaying near-identical singlet energies and PLQYs, the triplet energies – and subsequent TADF performances

– were markedly different and showed opposite trends as the D-A materials. Molecular orbital interactions with higher energy multi-donor LE states are responsible for these unexpected changes in triplet energy, with interaction strength modulated by the linkage patterns of the two donor subunits. The identification of these emergent multi-donor effects – not complicated here by any additional impacts of steric environment changes – demonstrates that bottom-up approaches to understanding TADF behaviour are unlikely to succeed. Due to different conjugation strengths across the linker unit for (*o,m*)ACA (*pD-D* state) than for (*o,o*)ACA (*mD-D* state), the *pD-D* state to be lower in energy and have larger electron density on the central bridge region. This would subsequently lead to a larger overlap between the *pD-D* state and the ³LE state associated with the A unit (3LEA) in (*o,m*)ACA as compared to *mD-D* in (*o,o*)ACA. The absorbance spectra showed the weak direct CT absorption bands in both (*o,o*)ACA and (*o,m*)ACA at ~375 nm. In each material this band corresponded to two closely spaced CT state absorptions, consistent with the DFT calculations and prior understanding of the *oDA* or *mDA* materials. In both cases this indicated that formation of the CT state involves only a single donor, and is unimpacted by the presence of the other.

5. Acknowledgements

This project was funded by the European Union (project No [S-ST-23-224], title “Artimo gamtai miškininkavimo modelių vystymas naudojant miškininkavimo sprendimų paramos sistemą Heureka”) under the agreement with the Research Council of Lithuania (LMTLT).

6. References

- [1] F. B. Dias, T. J. Penfold, A. P. Monkman, Photophysics of thermally activated delayed fluorescence molecules. *Methods Appl. Fluoresc.*, 5 (2017) 012001. doi:10.1088/2050-6120/aa537e.
- [2] C. S. Oh, D. D. S. Pereira, S. H. Han, H. J. Park, H. F. Higginbotham, A. P. Monkman, J. Y. Lee, Dihedral angle control of blue thermally activated delayed fluorescent emitters through donor substitution position for efficient reverse intersystem crossing. *ACS Appl. Mater. Interfaces* 10 (2018) 35420–35429. doi:10.1021/acsami.8b10595.

- [3] N. Ye, Z. Yang, Y. Liu, Applications of density functional theory in COVID-19 drug modeling. *Drug Discov. Today* 27 (2022) 1411–1419. doi: 10.1016/j.drudis.2021.12.017.
- [4] D. H. Kim, D. W. Kim, J. Y. Jang, N. Lee, Y. J. Ko, S. M. Lee, H. J. Kim, K. Na, S. U. Son, Fe₃O₄@void@microporous organic polymer-based multifunctional drug delivery systems: Targeting, imaging, and magneto-thermal behaviors. *ACS Appl. Mater. Interfaces* 12 (2020) 37628–37636. doi:10.1021/acsami.0c12237.
- [5] S. J. Woo, Y. H. Ha, Y. H. Kim, J. J. Kim, Effect of ortho- biphenyl substitution on the excited state dynamics of multi-carbazole TADF molecule. *J. Mater. Chem. C* 8 (2020) 12075-12084.
- [6] T. J. Penfold, E. Gindensperger, C. Daniel, C. M. Marian, Spin-vibronic mechanism for intersystem crossing. *Chem. Rev.* 118 (2018) 6975-7025.
- [7] M. J. Frisch, G. W. Trucks, H. B. Schlegel, G. E. Scuseria, M. A. Robb, J. R. Cheeseman, G. Scalmani, V. Barone, G. A. Petersson, H. Nakatsuji, X. Li, M. Caricato, A. V. Marenich, J. Bloino, B. G. Janesko, R. Gomperts, Gaussian, Inc., Wallingford CT.
- [8] T. Rangel, S. M. Hamed, F. Bruneval, J. B. Neaton, An assessment of low-lying excitation energies and triplet instabilities of organic molecules with an ab Initio bethe- salpeter equation approach and the Tamm-Dancoff approximation, *J. Chem. Phys.* 146 (2017) 194108-8.
- [9] J. J. P. Stewart, Optimization of parameters for semiempirical methods VI: more modifications to the NDDO approximations and re-optimization of parameters. *J. Mol. Model.*, 19 (2013) 1–32. doi:10.1007/s00894-012-1667-x.
- [10] M. K. Etherington, J. Gibson, H. F. Higginbotham, T. J. Penfold, A. P. Monkman, Revealing the spin–vibronic coupling mechanism of thermally activated delayed fluorescence. *Nat. Commun.*, 7 (2016) 1–7. doi:10.1038/ncomms13680.